

Nonlinear Dynamic Modeling of a Supersonic Commercial Transport Turbo-Machinery Propulsion System for Aero-Propulso-Servo-Elasticity Research

Joseph W. Connolly*, George Kopasakis†

NASA Glenn Research Center, Cleveland, OH 44135, USA

Jan-Renee Carlson‡

NASA Langley Research Center, Hampton, VA 23681, USA

Kyle Woolwine§

University of Colorado, Boulder, CO 80309, USA

This paper covers the development of an integrated nonlinear dynamic model for a variable cycle turbofan engine, supersonic inlet, and convergent-divergent nozzle that can be integrated with an aeroelastic vehicle model to create an overall Aero-Propulso-Servo-Elastic (APSE) modeling tool. The primary focus of this study is to provide a means to capture relevant thrust dynamics of a full supersonic propulsion system by using relatively simple quasi-one dimensional computational fluid dynamics (CFD) methods that will allow for accurate control algorithm development and capture the key aspects of the thrust to feed into an APSE model. Previously, propulsion system component models have been developed and are used for this study of the fully integrated propulsion system. An overview of the methodology is presented for the modeling of each propulsion component, with a focus on its associated coupling for the overall model. To conduct APSE studies the described dynamic propulsion system model is integrated into a high fidelity CFD model of the full vehicle capable of conducting aero-elastic studies. Dynamic thrust analysis for the quasi-one dimensional dynamic propulsion system model is presented along with an initial three dimensional flow field model of the engine integrated into a supersonic commercial transport.

Nomenclature

A	Cross-sectional area	η	Efficiency
N	Engine rotational speed	γ	Ratio of specific heat
M	Mach number	ρ	Density
P	Pressure	<i>Subscripts</i>	
PR	Pressure Ratio	c	Engine characteristic parameter
T	Temperature	n	Engine component location
V	Volume	s	Static flow condition
\dot{m}	Mass flow	t	Total flow condition
t	Time	v	Engine volume gas parameter
x	Length		

*Aerospace Engineer, Intelligent Control and Autonomy Branch, AIAA Senior Member

†Controls Engineer, Intelligent Control and Autonomy Branch, AIAA Member

‡Aerospace Engineer, Aero-Sciences Branch, AIAA Member

§Ph.D. Student, Aerospace Engineering Department

I. Introduction

NASA aims to overcome the obstacles associated with supersonic commercial flight by developing the technologies to allow for a practical overland supersonic commercial transport. The primary driver of this technology development is to reduce noise associated with the sonic boom. Thus, the proposed vehicles are long, slim body aircraft with the potential for pronounced structural vibrations that need to be controlled. The modeling and control of these structural vibrations is known as aero-servo-elasticity (ASE). NASA has investigated the ASE issue extensively using both computational and experimental methods in both the subsonic and supersonic flight regimes.^{1,2} A less explored aspect of the ASE field is how the vehicle structural dynamic response can be impacted by the propulsion system. When coupled with propulsion system dynamics, the structural modes excited by the aerodynamic flow field are known as aero-propulso-servo-elasticity (APSE). APSE considerations can lead to design challenges pertaining to aircraft performance such as aircraft ride quality and stability. Furthermore, other disturbances upstream of the inlet generated by atmospheric wind gusts may also affect performance. To study these phenomena, an integrated model is needed that includes both airframe structural dynamics and the propulsion system dynamics.

This paper takes a step along the way of achieving an overall APSE model by presenting the propulsion system nonlinear dynamic model comprised of an external compression inlet, variable cycle turbofan-engine (VCE), and convergent-divergent nozzles. Three variations of the propulsion system models will be presented. The first is a quasi-one-dimensional (quasi-1D) propulsion system model that serves as an environment to develop and test propulsion control algorithms, while gaining an understanding of the fundamental dynamic response of the system. The second, will couple the VCE portion of the quasi-1D model into a stand alone propulsion model in NASA Langley's Fully Unstructured Navier-Stokes in Three Dimensions (FUN3D) code.³ The FUN3D code has various configuration options to include tools outside of the standard flow solver. NASA is using FUN3D as the primary tool for computational fluid dynamics (CFD) based ASE analysis⁴ and it will serve as the analysis environment for the final APSE model. Finally, the stand alone propulsion system model will be coupled into a rigid body supersonic commercial transport in FUN3D.

Previously, the major components of the quasi-1D propulsion system used for this study were developed separately for the inlet, VCE, and nozzle.⁵ This paper leverages this past work to investigate the coupling of the full propulsion system using CFD modeling of the external compression inlet and nozzle, while using a lumped volume approach for the VCE. This level of fidelity for modeling the larger volume components of the propulsion system accurately captures the thrust dynamics required for the APSE task and provides greater confidence in the control algorithm development. Typically, quasi-1D CFD models of turbofan engines have not been necessary for control design of subsonic commercial aircraft due to their operating conditions of lower frequency flow field perturbations. For such models, only the shaft inertias have been required for controls development. Due to the higher frequency flow field perturbations the potential for vehicle-propulsion interaction necessitates higher fidelity modeling. The dynamic models presented here use simple quasi-1D finite difference and finite volume schemes to capture the gas dynamics not typically considered in control design of subsonic commercial turbofan engines.

The quasi-1D model is important for controls development and initial dynamic investigations; however, the main goal for this work is to create an overall APSE model that requires a three dimensional (3D) CFD model. To this end the VCE model will be incorporated into FUN3D. This is a widely used 3D CFD code, that is enhanced here to provide the capability of including turbo-machinery components. Only the VCE and portions of the internal ducts will be coupled from the quasi-1D model. FUN3D will handle the more complex external flows of the inlet and nozzle. The stand alone propulsion system model coupled with FUN3D will provide a more detailed dynamic thrust response, given its ability to model the external flows that are largely neglected using a quasi-1D approach. The quasi-1D model can provide initial comparisons to the stand alone FUN3D propulsion system, given the lack of any test data to verify the dynamic thrust response. However, for the initial coupling only steady-state solutions of the propulsion system in FUN3D are presented. The stand alone model is then coupled with a rigid supersonic commercial transport model that has previously been used in static aero-elastic analysis,⁴ but without the propulsion system. The structural modes used in the previous ASE analysis can be interpolated to the supersonic commercial transport with the propulsion system to ultimately obtain the APSE model.

While integrated propulsion system dynamic models have been developed in support of previous NASA supersonic projects by Garrard,⁶⁻⁸ Gamble,⁹ Numbers,¹⁰ and Giannola,¹¹ the distinction in the work that is presented here provides a platform for coupling into an ASE vehicle model. This paper will first provide an overview of the supersonic commercial transport and the need for this model in the context of APSE

studies. Then a synopsis is provided for the modeling approach of the previously developed major propulsion components of the inlet, gas turbine engine, and nozzle, along with their associated coupling. The individual component models have been compared to test data where available and other models when test data is lacking. Some additional verification against higher fidelity codes is provided here. The VCE model is integrated into the FUN3D code for the overall supersonic commercial transport with propulsion system. Finally, studies of the propulsion system thrust dynamics from the quasi-1D model and initial results of the flow field for the engine model incorporated into the FUN3D code are presented to show feasibility of the ultimate APSE modeling tool.

II. Supersonic Commercial Transport Overview

To address future challenges in aerospace, NASA has a technology development approach to advance modeling tools and capabilities based on future generations of aerospace vehicles. Under the NASA two generations from present state (N+2) design, Lockheed Martin has developed a low-boom supersonic configuration illustrated conceptually in Fig. 1.⁴ The key features to note for this study are the long slender vehicle profile and the three gas turbine engines. Two of the engines are mounted under the wing, with a third along the centerline of the fuselage. The two engines mounted under the wing are close to the fuselage and may offer some relief from possible aeroelastic issues as opposed to the engines being traditionally mounted further out on the span of the wing. However, having these large masses located at the tail of a flexible fuselage may lead to aeroelastic issues.⁴



Figure 1. Artistic concept of the Lockheed Martin N+2 commercial supersonic transport vehicle.

The general characteristics of the N+2 configuration are listed in Table 1. As a comparison of the N+2 configuration to the previous supersonic commercial transport, the Concorde, the N+2 configuration is about 21% longer. Yet, it has approximately the same wingspan. The primary difference is the lower cruise Mach number of 1.7 compared to that of the Concorde cruise Mach number of 2. One of the drivers for the lower flight speed is to reduce the complexity of lowering the sonic boom signature, and thus allow supersonic flight over land.

Table 1. The basic geometric, weight, and cruise operating condition of the N+2 commercial supersonic transport.

Geometry		
Length	Span	Height
244 ft	83 ft 10 in	30 ft 6 in
Weight		
Take Off	Fuel	Empty
320,000 lbs	168,000 lbs	136,000 lbs
Cruise Operating Condition		
Altitude	Mach	Angle of Attack
50,000 ft	1.7	2.25 deg.

III. APSE Model Overview

The overall APSE model block diagram can be seen in Fig. 2, where the propulsion system is highlighted and is comprised of the external compression inlet, VCE, CD nozzle, and associated controllers. The aero-elastic vehicle impacts are not included in this study. Both the vehicle and propulsion system are directly impacted by the freestream flight conditions, which have the capability to be time varying to simulate atmospheric turbulence or alteration of the vehicle angle of attack. The propulsion system and aero-elastic vehicle will have two primary interfaces. The first being variations of the vehicle or propulsion system that impact the surrounding flow field. This includes vehicle wing vibrations that subsequently induce perturbations into the flow field in front of the mounted propulsion system and the propulsion system inlet shock field and nozzle exit plume impact on the vehicle. The flow field perturbations are all captured within the CFD approach and are illustrated by solid lines. The second interface of the APSE model is the thrust perturbations that have the potential to induce additional or accentuate current structural modes through their force oscillation on the vehicle pylons. This interface will require improvements to the current finite element model of the vehicle and is illustrated by a dashed line.

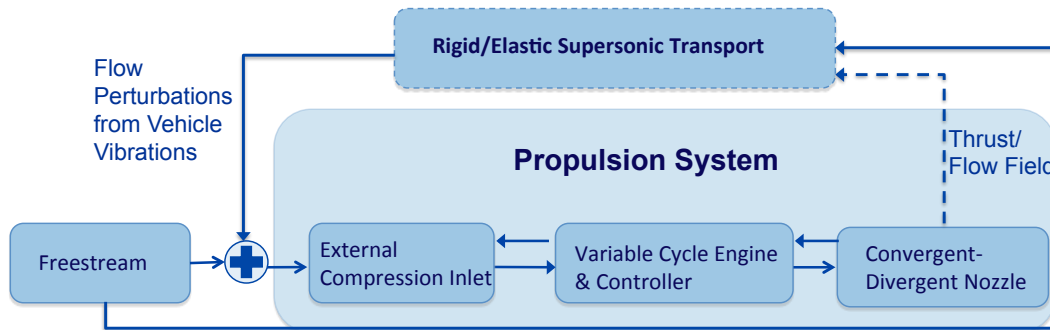


Figure 2. Block diagram of overall APSE system model with propulsion system highlighted.

As discussed, an overall goal of the ASE project is to integrate a high fidelity vehicle and propulsion system model to investigate the dynamic performance coupled with the elastic vehicle. The work presented here is a step along that path, providing improved dynamic thrust estimation and the full engine model integrated into the FUN3D code that is capable of aero-elastic studies. Previous work in the area of APSE has focused on either the vehicle or the propulsion system, but rarely are both systems modeled with the same level of fidelity.¹²⁻¹⁴

IV. Quasi-1D Propulsion System Modeling

The current project design calls for an external compression inlet as opposed to previous commercial supersonic commercial vehicles that were considering mixed compression inlets. All of the propulsion components are modeled using unsteady Euler conservation equations, described in the following sections and previous publications.^{15,16} This allows for the investigation of both propulsion system control performance and thrust oscillations. The new addition here is the coupling of all of the component models into an overall quasi-1D propulsion system model. Freestream static conditions of pressure, temperature, and Mach number are applied to the applicable performance calculations to obtain the flow conditions at the internal duct portion of the inlet. At this point, conservation equations are applied to model the inlet internal duct dynamics to obtain the total pressure and temperature at the engine face input conditions. The engine then uses the input conditions, component performance maps, and a modified version of the Euler conservation equations to calculate the engine output provided to the CD nozzle interfaces. Conservation equations are used for the nozzle for the internal duct portion. The following subsection will highlight the component models previously developed, and discuss the coupling of the new quasi-1D propulsion system model.

A. Inlet Modeling

The inlet is modeled using a quasi-1D implementation of the Euler equations for the internal duct portion. For the portion of the flow between the centerbody tip and the internal duct, established oblique shock equations are used, which determine the pressure recovery and Mach number.^{15,16} This is done assuming that the external flow is much faster than the internal duct, where the dynamics will dominate the response. The CFD approach uses a MacCormack scheme applied to non-dimensional Euler conservation equations.

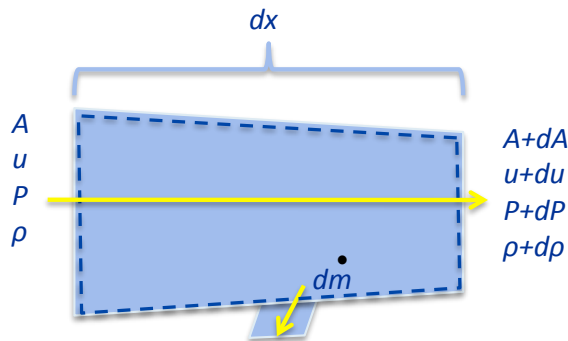


Figure 3. Quasi-1D flow representation of differential volume.

prescribed. The supersonic cruise profile described for the N+2 concept vehicle is used for this study. The inlet subsonic outflow boundary is defined by setting the inlet exit back pressure, while the other two flow variables are calculated using a characteristic boundary condition.¹⁸

Quasi-1D modeling of a supersonic inlet has previously been done using this methodology for a mixed compression¹⁵ and external compression inlet.¹⁶ Inlet tests were conducted at NASA Glenn Research Center in the 8x6 wind tunnel.^{19,20} It was shown that there was some error in capturing the external normal shock using the described method; however, once the model was no longer dominated by the error of the external shock, it captures the static pressure distribution reasonably well for the internal duct. Research is ongoing to develop better models of the external flow of the axi-symmetric external compression inlet. The primary difficulty is accurately capturing the flow spillage change due to perturbations. The focus of the results presented here is on the internal duct, as this will serve as the basis for the scheme developed to improve the external flow dynamic modeling.

B. Gas Turbine Modeling

The gas turbine engine comprises another major element of the overall propulsion system. Initially, the modeling efforts used a turbojet engine similar to the General Electric J-85 for verification as dynamic experimental data was available.²¹ Since the feasibility was shown with the J-85, more relevant supersonic engine concepts such as the VCE will be considered here.

Variable Cycle Engine Design Concept

The current engine design concept of the supersonic propulsion system is a VCE. The flow coming from the inlet goes through the fan component and is split into three gas paths as illustrated in Fig. 4. The primary gas path is nearly identical to the turbojet and goes through the core of the engine. The secondary gas path is similar to a typical turbofan engine in that a large amount of the flow is bypassed around the core of the engine. This secondary flow has its own nozzle downstream of the bypass duct. The third gas path exhausts through its own nozzle in a similar manner to the primary fan flow. This path provides a lower exit velocity that could be used as a noise shield for the flow exiting the core nozzle.

Compressive Component Modeling Example

A schematic of the modeling approach can be seen in Fig. 3, where over a small distance, dx , the fluid properties change by a differential amount.¹⁵ The governing equations are implemented in the model assuming that the inlet geometry is fixed. This is acceptable because geometry conditions change very slowly when compared to the fluid flow. The model is integrated numerically using MacCormack's method.¹⁷ In the vicinity of shocks, an artificial viscosity term is included to dampen out non-physical oscillations. The artificial viscosity coefficient is carefully chosen such that dampening occurs, but the associated diffusion does not significantly degrade the accuracy of the numerical scheme.

The inlet freestream boundary condition is supersonic, thus all aspects of the flow field are directly

The gas turbine engine model uses a single lumped volume for each of the major components such as fan, compressors, combustor, and turbines. The modeling approach is outlined in Seldner²² and refined in Kopasakis.²¹ A schematic for a compressive component is defined here for completeness and for understanding the level of fidelity of the non-linear model, which is coupled into the overall propulsion model. Most of the geometric information for the engine is obtained from the engine cycle design code, Numeric Propulsion System Simulations (NPSS) models.²³ Each of the fluid flow components is modeled using a set of derived conservation equations modified from the standard Euler form and written as continuity, momentum, and energy. These equations are integrated numerically using a trapezoidal time marching scheme and the Seldner differencing technique of the spatial terms.²¹

A general schematic of the overall modeling approach for the compressive component can be seen in Fig. 5. This schematic is analogous to the other major components, with the exception of the performance map, which may or may not be required to meet characteristic flow parameters. The incoming flow conditions are used with performance maps to generate characteristic values for this particular engine design. The performance map is actually two table lookups in the model, which provides pressure ratio and efficiency as functions of corrected flow and shaft speed. These are then used to get the characteristic pressure and temperature. Since this is a subsonic system, information travels in both directions along characteristic lines. The spatial differencing of the governing equations is illustrated by the subscript n that indicates the current component and are linked together by the equation of state. The three state variables chosen for the model of each component are the static density, static density times the total temperature, and mass flow rate. The Seldner method used here, which compares well with test data,²¹ uses a unique spatial differencing. Work is ongoing to verify if the matching of the method to test data is primarily the result of the inertia dynamics, or if the unique spatial differencing is able to capture the relevant gas dynamics.

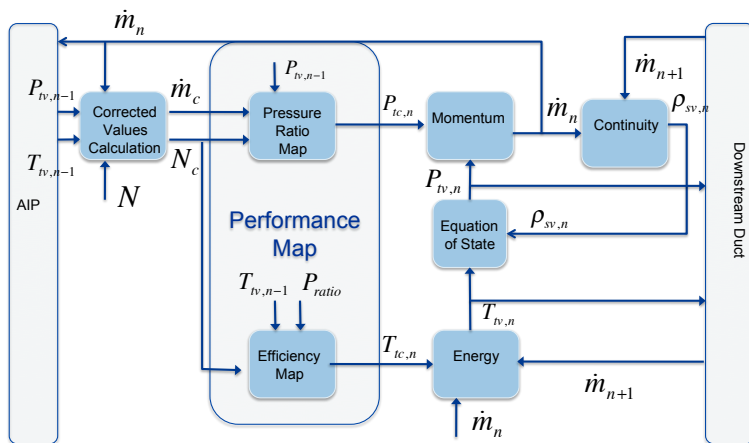


Figure 5. Gas turbine engine compressive component modeling schematic.

In the current study, the flight controller is neglected since the focus is on the cruise flight condition and the flight control surfaces are not expected to change significantly. However, the engine controller is included

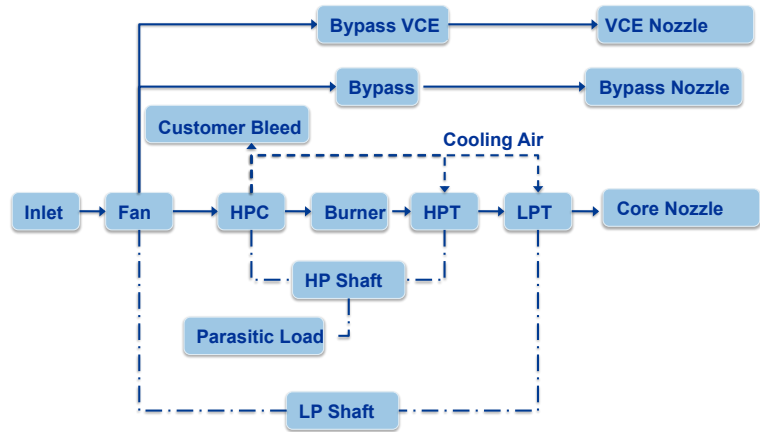


Figure 4. Main components of design concept for a variable cycle engine.

A cruise operating point was chosen at 15,240 m (50,000 ft) and a Mach number of 1.7. The nozzle exit boundary is obtained by assuming that the flow is choked at the nozzle throat, and the expansion of the flow in the divergent portion of the nozzle is ideal isentropic flow with no internal shocks. The main parameter of interest for this study is the thrust, because it is the feedback parameter when the propulsion system is coupled with the vehicle model. It is calculated here as the gross thrust, which deviates from NPSS calculations by only about 1%.¹⁵

Control System and Disturbances

For the full APSE model, controllers will eventually be required for both the flight vehicle and propulsion system. In the

here to add stability to the propulsion system model. The engine control design used here has aspects of classical loop shaping²⁰ design and Quantitative Feedback Theory.^{24,25} The fan shaft speed is controlled using the engine fuel injector that has a bandwidth of 6 Hz. An important note is that the bandwidth of approximately 6 Hz for a fuel injector will not be able to attenuate disturbances in the tens of hertz that are expected from atmospheric turbulence at supersonic cruise.^{26,27} The highest expected frequency due to atmospheric turbulence at the desired cruise condition of Mach 1.7 is about 20 Hz. The atmospheric disturbances will be used to provide expected freestream perturbations for the integrated quasi-1D propulsion system. In addition to the atmospheric disturbances, the APSE model aero-elastic disturbances due to the vehicle vibrations may perturb the flow field at frequencies up to 60 Hz. Mitigation of disturbances this high in frequency will require use of the flight control surfaces. By knowing the expected disturbance frequency range is up to 60 Hz, it provides information that the required system dynamic response frequency range is up to 600 Hz, or a decade above the highest frequency disturbance.

C. Nozzle Modeling

A Convergent-Divergent (CD) nozzle component model was developed to improve the dynamic thrust response caused by upstream flow perturbations at the engine-nozzle boundary.²⁸ As previously mentioned, the VCE propulsion system has three nozzles. All of the nozzles are modeled exactly the same with different geometries. The nozzles chosen for the supersonic transport include a variable geometry CD internal duct and a conical plug or center body. The CFD approach chosen is the same as that discussed for the inlet. Thus, the approach is only suitable to model the internal duct portion of the nozzles and neglects any effects of the external plug. This approach is justified by preliminary studies using a two-dimensional code that showed that the external portion of the nozzle only contributed a few percent to the overall thrust.²⁹

At the nozzle subsonic inflow boundary, one of the boundary condition variables is required to float, since information under this condition traverses both upstream and downstream. The choice was to allow the velocity to float. The boundary conditions are then defined in terms of the solution vector, where the density and temperature at the nozzle entrance are prescribed. The boundary conditions at the nozzle exit are extrapolated using a characteristic equation, since the flow is assumed to have no internal normal shocks, and thus be supersonic. Previously, a steady-state and unsteady solution of the core nozzle were investigated spanning the frequency range of interest that resulted in good agreement with another quasi-1D method.²⁸

D. Propulsion Component Coupling

A complete propulsion system model has the inlet model coupled with the gas turbine and nozzle models. The integrated nonlinear propulsion system used in this study includes an external compression inlet, a VCE, and CD nozzle models. This will allow for the accurate capturing of dynamic thrust and a means to develop the required control algorithms. The boundary conditions used for the quasi-1D models for the interfaces between the individual components are the same as those used for the coupling of the VCE into FUN3D. The main exception is that the 3D flow field is averaged to a single value to pass across the inlet-engine boundary and the engine defines a uniform 3D flow field at the engine-nozzle boundary.

1. Inlet to Engine

The engine requires total pressure and total temperature from the FUN3D subsonic outflow boundary. The coupling approach used standard engine model input boundary conditions with minor changes to the existing subsonic outflow boundary condition in FUN3D.³⁰ This approach reduced some of the modifications required in FUN3D. The aerodynamic interface plane (AIP) or the exit boundary condition of the inlet is typically the most stable in FUN3D, if a prescribed static pressure for the subsonic outflow is used. Therefore, in FUN3D the static pressure is specified for this outflow boundary condition and the velocity and temperature are extrapolated. Since this is a subsonic outflow boundary interfacing with a 1D code, two flow values are extrapolated and one is defined at the boundary of the engine-inlet interface. To interface with the engine library, the 3D values are averaged to a single axial value. These mean values are then used to calculate the total pressure and temperature at the engine-inlet boundary. The engine library then uses the calculated mass flow rate at the engine-inlet boundary to update the specified inlet back pressure.

A duct volume is modeled prior to the turbo-machinery components in the engine library to calculate the described flow variables at the inlet-engine boundary, where the conservation equations become Eqs. (1)

to (3).

$$\frac{d}{dt}(\rho_s) = \frac{1}{V}(\dot{m}^{inlet_{exit}} - \dot{m}^{engine}) \quad (1)$$

$$\frac{d}{dt}(\dot{m}) = \frac{A}{x}(P_s^{inlet_{exit-1}} - P_s^{inlet_{exit}}) \quad (2)$$

$$\frac{d}{dt}(\rho_s T_t) = \frac{\gamma}{V}(T_t^{inlet_{exit-1}} \dot{m}^{inlet_{exit}} - T_t^{inlet_{exit}} \dot{m}^{engine}) \quad (3)$$

The superscripts used in the above equations indicate the location of the variable relative to the AIP and engine face. These equations are then tied together using the state equation to obtain the inlet exit state variables for the downstream engine face and the upstream inlet grid points.

2. Engine to Nozzle

A similar approach to that described for the inlet-engine boundary is used here for the engine-nozzle boundary. Here the engine library outputs the total pressure and temperature to the upstream nozzle, while awaiting information about the mass flow to be passed downstream from the FUN3D nozzle model. The modeling of this interface is accomplished by modifying the FUN3D subsonic inflow boundary condition. For the subsonic inflow boundary condition, two flow values are defined and one is extrapolated. Again, the 3D values are averaged to a single 1D axial value. Here the engine library defines the total pressure and temperature for the nozzle plenum uniformly across the boundary, while the boundary was modified to pass the mass flow information back to the engine model. It should be noted here that with the engine library being a 1D model, any flow distortion in the inlet is simply averaged out at the nozzle interface. The mass flow coming from FUN3D replaces a previous simple choked flow boundary condition in the engine library with a very small duct volume added at the exit of the engine library. This duct volume is modeled using volume dynamics, in a similar manner to that of the inlet-engine interface above, since both interfaces are subsonic.

V. Propulsion System Model for APSE Studies

A. Stand Alone Propulsion System Model in Fun3D

To conduct APSE studies, the propulsion system model needs to be integrated into a Navier-Stokes solver that is capable of modeling aero-elastic effects of a commercial supersonic vehicle, such as FUN3D. Up until now, FUN3D could simulate inlet and nozzle flows, but not the effect of any turbo-machinery components that may influence those flows. The inclusion of the VCE engine will provide a new capability by creating a C code library of the engine model that can be called by FUN3D. The previously developed quasi-1D approach for the inlet and nozzle is replaced with the higher fidelity CFD tool. Two model coupling efforts with FUN3D have been done for this study and described in the following sections. Initially, a stand alone engine test model was developed that includes the complicated three stream nozzle flow path. This current proof-of-concept configuration is a fully 3D engine nacelle with an external compression axi-symmetric inlet and a three-flow path CD nozzle. These two external component models are connected by the quasi-1D C-library VCE model. The engine model uses the average total pressure and temperature from the solution at the inlet face coming from the 3D flow solver and calculates the nozzle inflow boundary conditions as discussed previously.

The engine library is called on each of the global time steps, where the library can execute using a defined time step for steady-state results or use the FUN3D time step to run time accurate models. A flow chart of the propulsion system model coupling into FUN3D is shown in Fig. 6. The primary functions are shown in flow chart blocks with a bold border. The sub-functions are smaller blocks without a bold border. The standard initialization begins a typical FUN3D execution with the coupled engine. The boundary conditions are then all defined. A new subroutine, *setup engine* was created here. This subroutine calls the engine model modules to define the current boundary condition values. The *engine interface* serves as the primary function that passes data between the Fortran and C codes. This is accomplished through the subroutine *get plenum data*. This function for the inlet-engine passes the total conditions of the pressure and temperature to the engine and the mass flow from the engine to update the back pressure inlet boundary condition. At the engine-nozzle interface the total pressure and temperature are passed to update the FUN3D subsonic

inflow boundary and the mass flow is provided back to the engine model. The *simulate engine* function calls the C engine library to use the boundary information passed by *engine interface*. The process of passing information across the engine boundary is conducted on every global time step of FUN3D for the duration of the model.

B. Propulsion System Model with Rigid Body Supersonic Commercial Transport

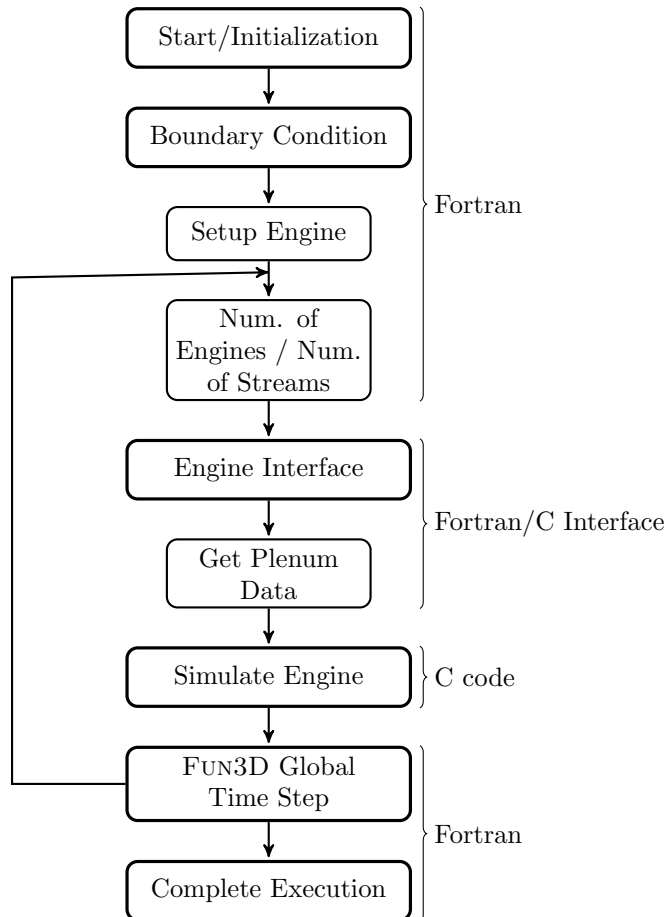


Figure 6. Fun3D software flow chart for engine library coupling.

The final propulsion system model implementation with FUN3D, is for the engine model included in a rigid semi-span model of the N+2 commercial supersonic transport. For the coupling into the full vehicle, a previously developed grid for the vehicle with hollow engine nacelles was used as a starting place. Then the grid of the hollow engine nacelle is replaced with the axi-symmetric inlet cone.^{15,16} While the baseline VCE propulsion system has three nozzles, coupling with the vehicle configuration was altered to simplify the mesh generation of the exit nozzle into the higher fidelity CFD tool. The three separate flow fields are now mixed into a common volume within the turbo-machinery model before exiting a single nozzle with the associated expansion plug. The previous design used the separate nozzle streams to shield the very high speed flow exiting the core of the engine with the slower larger mass flows of the bypass streams. This will alter the exit nozzle plume from the current design configuration, but it should still capture the relevant physics of the problem and general trends of including the propulsion system into an ASE study. This change in the grid is shown in Fig. 7. The previous mesh is illustrated as a grey shaded feature and the additional propulsion components are illustrated as a black mesh. Boundary planes are inserted into the mesh for the engine to interface with FUN3D as was described.

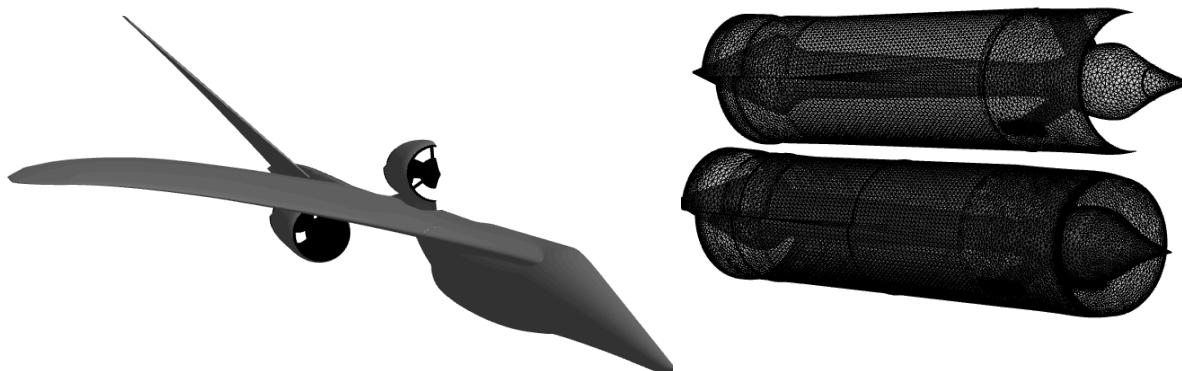


Figure 7. Unstructured grid of the N+2 vehicle with external propulsion system components.

VI. Results

The results will be broken out into three sub-sections; one for the stand-alone propulsion system component models, one for the fully integrated quasi-1D propulsion system, and one for coupling of the VCE model with FUN3D. The subsections for the individual component models will provide comparisons of the quasi-1D modeling technique to more advanced 2D CFD models. The quasi-1D integrated model subsection will focus on thrust dynamics of the propulsion system due to upstream flow perturbations. Finally, some results of the VCE engine integrated into the three-dimensional FUN3D code are also provided. The results presented are focused around supersonic cruise, which for this activity is in the Mach 1.6-1.8 range at an altitude of 50,000 ft.

A. Quasi-1D Propulsion System Component Modeling Verification

External Compression Axi-Symmetric Inlet

The focus here is only on the internal portion of the inlet where the dynamics of the system will be modeled. This inlet is only a concept currently, thus results can only be compared to other models. The comparison is done with the Parallel Hierarchic Adaptive Stabilized Transient Analysis (PHASTA) code.³¹ This code uses a streamline upwind/Petrov-Galerkin finite element method for the spatial discretization and an implicit second order generalized-alpha method for time. The result shown in Fig. 8 illustrates that the two codes compare well. The inlet cowl is represented at the 0 length and the engine face is located at 1. The PHASTA code is being executed as a quasi-3D mode here, where the axisymmetric inlet is represented as 2D with a one degree wedge of the overall inlet. The flow parameters are averaged across the height of the inlet to compare to the quasi-1D code. An additional constant area length is added downstream of the engine face to allow dynamic model data to be captured at the engine face without being impacted by the subsonic outflow boundary condition of pressure. The condition here is considered super critical where the normal shock is just inside of the duct.

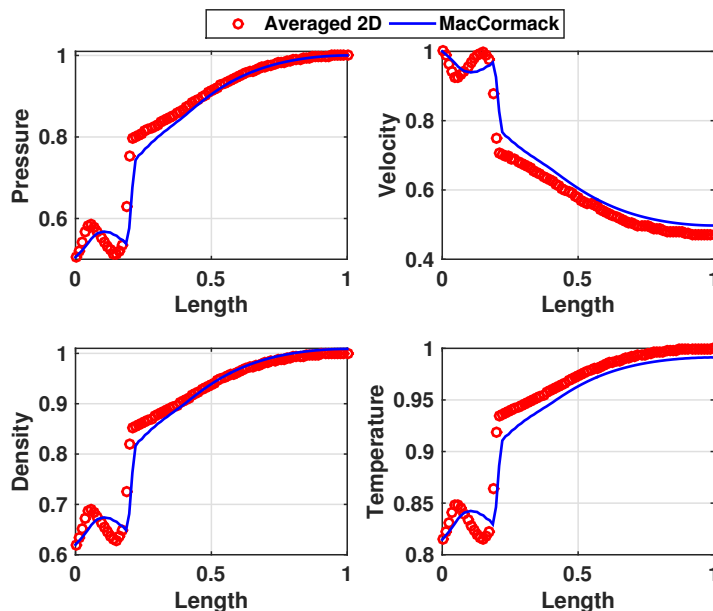


Figure 8. Supersonic inlet internal duct steady-state inviscid comparison of Quasi-1D MacCormack to 2D PHASTA code.

to be captured at the engine face without being impacted by the subsonic outflow boundary condition of pressure. The condition here is considered super critical where the normal shock is just inside of the duct.

The codes are able to capture the shock location nearly at the same location, just inside the inlet cowl shown by the normalized flow variables of pressure, temperature, density and velocity. The greatest errors are the discrepancies just before the normal shock, where the PHASTA code captures some 2D effects of the inlet at the cowl entrance. The quasi-1D code averages out the sharper changes that the PHASTA code illustrates prior to the shock.

To illustrate the dynamic comparison of the two codes a 22 Hz pressure sinusoidal disturbance was applied to the freestream condition where the time response is shown in the left of Fig. 9. The same type of disturbance is applied at higher frequencies to obtain the Bode plot shown in the right of Fig. 9. The two points of interest for the inlet are the duct entrance at the cowl and engine face. The flow values from PHASTA at the cowl serve as the input boundary conditions for the quasi-1D code. Shown in Fig. 9 is the normalized pressure disturbance with the steady-state removed in green. The pressure response at the engine face is then shown for the quasi-1D code in blue, and an averaged 2D pressure value is shown as a dashed red line. The comparison of the dynamic time response between the two codes shown in the left hand side of Fig. 9 is excellent with the two responses being nearly identical. The higher frequency comparison

of the two codes is shown as a Bode plot in the right hand side of Fig. 9, with the quasi-1D results in blue and PHASTA results in red. Here, the results again show a nearly identical response until about 1000 Hz, where there exists a slight offset in the magnitude.

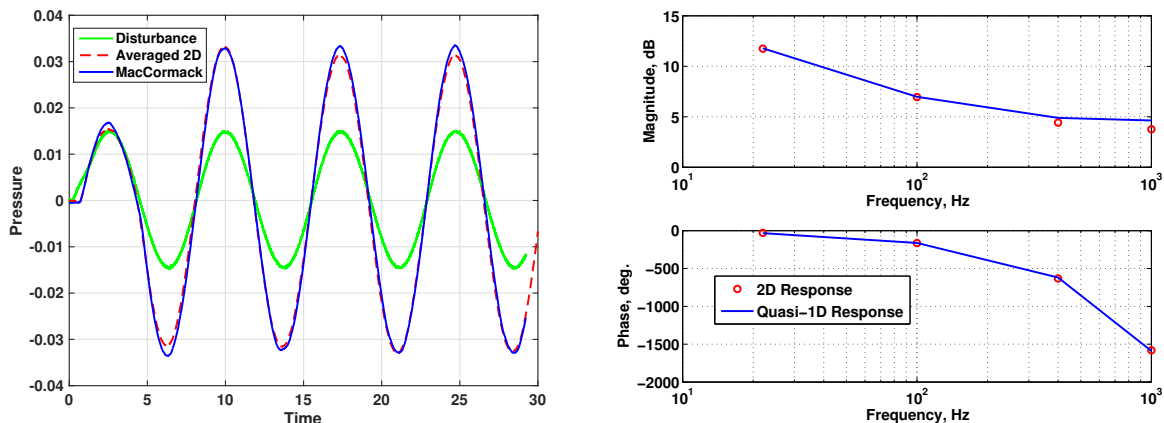


Figure 9. Inlet model exit pressure time response to freestream pressure disturbance of 22 Hz (left) and Bode plot using individual pressure sine wave disturbances in a frequency range of 22 to 1000 Hz (right)

Nozzle

To compare the dynamic accuracy of the nozzle model, results are compared to a more complex two-dimensional Computation Element Solution Element (CESE) model.³² Previously, preliminary comparisons were made using simple quasi-1D codes. The CESE method is a second-order accurate method. A guiding principal of the CESE formulation is that space and time are unified and time is simply treated as an additional dimension to the problem. In addition, the enforcement of flux conservation in space and time at an interface is an integral part of the solution procedure. A nozzle input using a density sinusoidal disturbance is applied to the subsonic inflow boundary and compared to the nozzle supersonic outflow boundary density response. The sinusoidal disturbance is applied across a frequency range of interest spanning 1-600 Hz. The input to output response is used to generate a Bode plot of the quasi-1D method compared to the 2D CESE method shown in Fig. 10. It can be seen that two methods agree very well, and provide a high level of confidence of the nozzle dynamics in the absence of experimental data. The results show that there is some discrepancy in the magnitude over 100 Hz, however the critical frequency range of interest is 60 Hz and below based on expected disturbances.

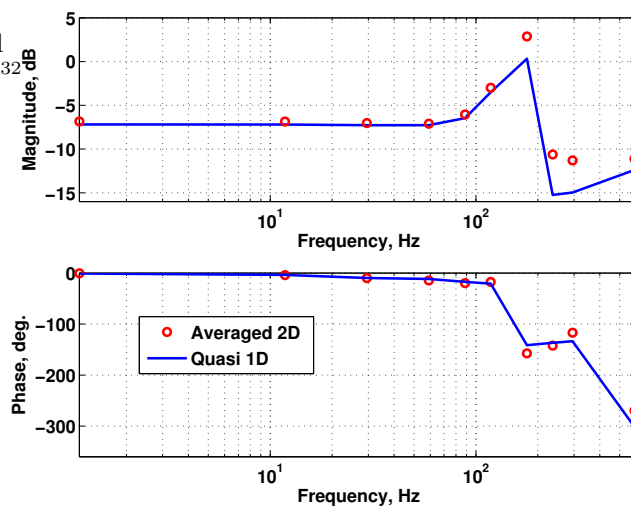


Figure 10. Comparison of quasi-1D and averaged 2D model results of a nozzle Bode plot of density sinusoid at entrance and corresponding response at exit.

B. Integrated Quasi-1D Propulsion System Model

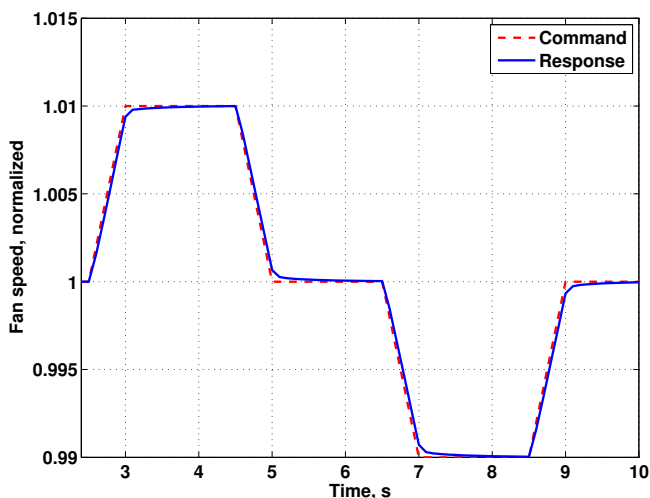


Figure 11. Engine-nozzle fan speed commanded steps and corresponding fan speed response.

dashed red line here is the commanded fan speed and the solid blue line is the response of the fan speed. This modest control demand is just used to illustrate that the propulsion system can operate about and maneuver around the cruise operating condition.

The fully integrated propulsion system is simulated for the above described cruise condition and compared against just the VCE model to illustrate the dynamic response change for the fully integrated model. For each model an upstream pressure disturbance of 1% is applied using a logarithmic sinusoidal sweep, similar to that used in the component model verification sections. The sinusoidal sweep spans the frequency range of interest from 1 to 600 Hz. A Bode plot of the thrust response to the pressure disturbance of only including the VCE is shown in Fig. 12 as a blue line. The corresponding integrated model Bode plot is shown as red circles. The frequency response illustrates a generally more complicated response than a second order response that is typically used as an initial approximation for turbo-machinery dynamics. The general trend is similar in nature to previous dynamic results that use this method for a turbojet engine.²¹

The inclusion of the inlet and nozzle does alter the shape of the frequency response in both magnitude and phase as shown in Fig. 12. However, the dominate change in the frequency response is the shift in the roll off of the coupled propulsion system to about 100 Hz instead of the 55 Hz of the VCE only.

For the second test case an atmospheric disturbance is applied to the upstream boundary condition of the inlet. The dynamics of the quasi-1D model start at the inlet internal duct and propagate the disturbance

The following section will outline the fan speed control response and the gross thrust response due to upstream flow perturbations, and results are presented for the VCE model integrated with the external compression inlet and three distinct convergent-divergent nozzles. The engine controller is critical for dynamic operation of the propulsion system, but it will not provide significant thrust oscillation suppression due to the actuator bandwidth being only about 6 Hz. Thus, unable to dampen the high frequency disturbance from turbulence and structural vibrations expected to range from 20 to 60 Hz. The results presented here are for a cruise condition of Mach 1.7, 50,000 ft, and 100% power.

A simple series of commanded fan speed steps up and down with a percent change of 1% from nominal are used to illustrate the controlled response and are shown in Fig. 11. The commands are applied after 2.5 seconds to allow for the startup transient to settle out. The

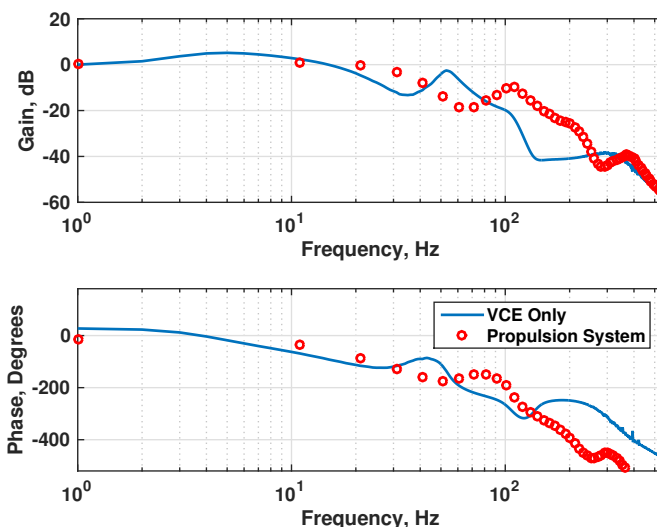


Figure 12. Thrust Bode plot response due to logarithmic pressure disturbance for the fully integrated dynamic model compared to only applying the disturbance to the VCE.

to the engine fan face. The engine fuel flow controller then attempts to modulate the fuel flow to maintain a constant fan speed, but it is not able to react to the higher frequency atmospheric disturbance. The disturbance is ultimately passed to the convergent divergent nozzles to obtain the resulting thrust response.

The atmospheric disturbance will perturb all of the incoming states, such as velocity, pressure, and temperature; however, only the temperature is shown for reference in Fig. 13 as it tends to dominate the thrust response. This turbulence upstream is mild with an eddy dissipation rate of 10^{-6} , which governs the magnitude of the disturbance. For reference, a typical atmospheric turbulence might use an eddy dissipation of 10^{-4} to simulate about four times the typical average. The smaller value is chosen for this study to illustrate the transient response of the thrust resulting from a couple percent magnitude change in the free stream boundary conditions. The resulting thrust percent change response is shown in Fig. 13.

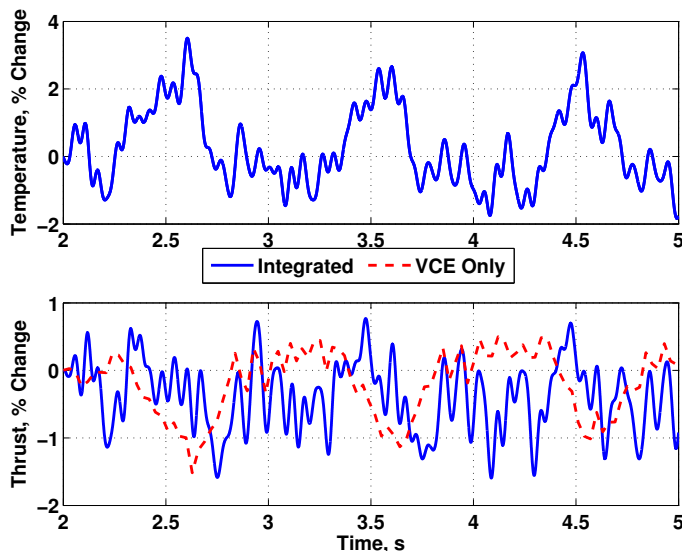


Figure 13. Thrust response due to atmospheric turbulence for the fully integrated dynamic model compared to only applying the disturbance to the VCE.

The thrust responses of the integrated propulsion system and the VCE are compared when the atmospheric disturbance is applied to the upstream boundary condition, as was done in previous work.¹⁵ Here, the integrated system exhibits a more complex dynamic response, however the magnitude of the thrust change is similar to the engine alone. This preliminary result indicates that to estimate the magnitude of the thrust change a relatively simple model can be used, but to capture all of the dynamic response the simple model will miss some of the transient features.

C. VCE coupling into Fun3D to Enable APSE Studies

A three dimensional model of the external compression axi-symmetric inlet is modeled with the three flow paths. To study APSE effects the VCE is integrated into FUN3D as a C library call. Previously, propulsion systems in FUN3D just modeled the gas turbine engine as a hollow tube. This new feature now allows accurate propagation of the flow condition at the inlet-engine boundary to the engine-nozzle boundary. Two implementations of the propulsion system in FUN3D are shown. The first is the stand alone model of the propulsion system. The second is the propulsion system integrated with the N+2 supersonic commercial transport.

Stand Alone Propulsion System

A steady-state solution of the Mach number contours is shown in Fig. 14 for the stand alone propulsion system. This preliminary result illustrates the Mach 1.7, 50,000 ft, and 100% power condition and exhibits the expected main features of the flow field with a normal shock near the inlet cowl and the nozzle flow capturing the complex interactions of the various speed of the flow exiting the three nozzles. The stand alone

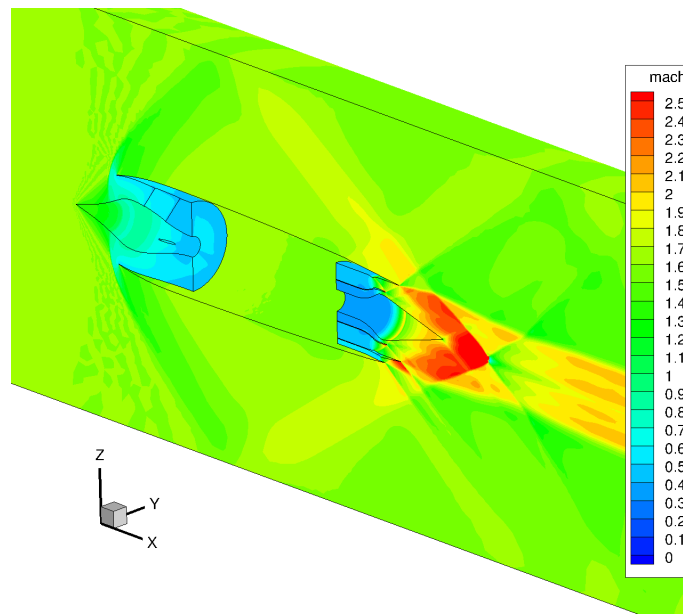


Figure 14. Fun3D propulsion system model with VCE lumped volume model steady-state Mach profile with three stream nozzle.

model was used as an initial test platform for the coupling, however the ultimate goal is to interface with the vehicle. Due to complications previously discussed with the grid development, the propulsion system configuration was changed to have a single exit nozzle. To accommodate the single exit nozzle the three exit flow streams in the VCE are mixed in a common duct prior to exiting the new nozzle. A simple two dimensional (2D) model of this configuration of the propulsion system was developed for testing purposes. The Mach contours for the new model are shown in Fig. 15. Given the change to the simple nozzle, on going work is needed to gain confidence in the results. However, the main goal of interfacing the two model environments was achieved. Further adjustments to the VCE propulsion system with a single nozzle may be required to supply adequate total pressure and temperature to accelerate the flow through the new nozzle.

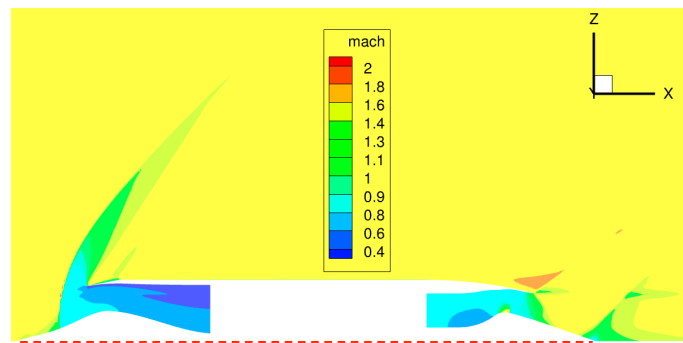


Figure 15. Fun3D propulsion system model with VCE lumped volume model steady-state Mach profile with simple nozzle, where red dashed line denotes axis of symmetry.

Propulsion System Integrated with Rigid N+2 Supersonic Commercial Transport

Currently, the full propulsion system has been integrated into the N+2 vehicle for a stable steady-state solution. A front view of the N+2 vehicle total pressure profile at the propulsion system inlet and the coefficient of pressure across the vehicle surfaces is shown in Fig. 16. The initial steady state solution integrated with the vehicle is a critical step, as this can help define the expected flow field entering the propulsion system. The flow field for the propulsion system under the wing was found to experience a

greater degree of distortion than the fuselage mounted engine. The full vehicle steady state solution is for illustrative purposes, while a close up view of the inlet-engine boundary for the propulsion system under the wing is shown Fig. 17 is of primary interest for this study. The normalized total pressure color scale shown is consistent between the two figures. The current configuration of the engine library will simply average out the distortion shown here; however, work is on going to add distortion capability to the VCE.⁵ The model presented here without distortion should still be able to capture the dominate thrust dynamics. The significantly larger amount of distortion entering the engine under the wing could indicate that the simplified nozzle used for coupling with the vehicle might require further redesign of the VCE propulsion system to provide a closer match to the expected conditions of the nozzle.

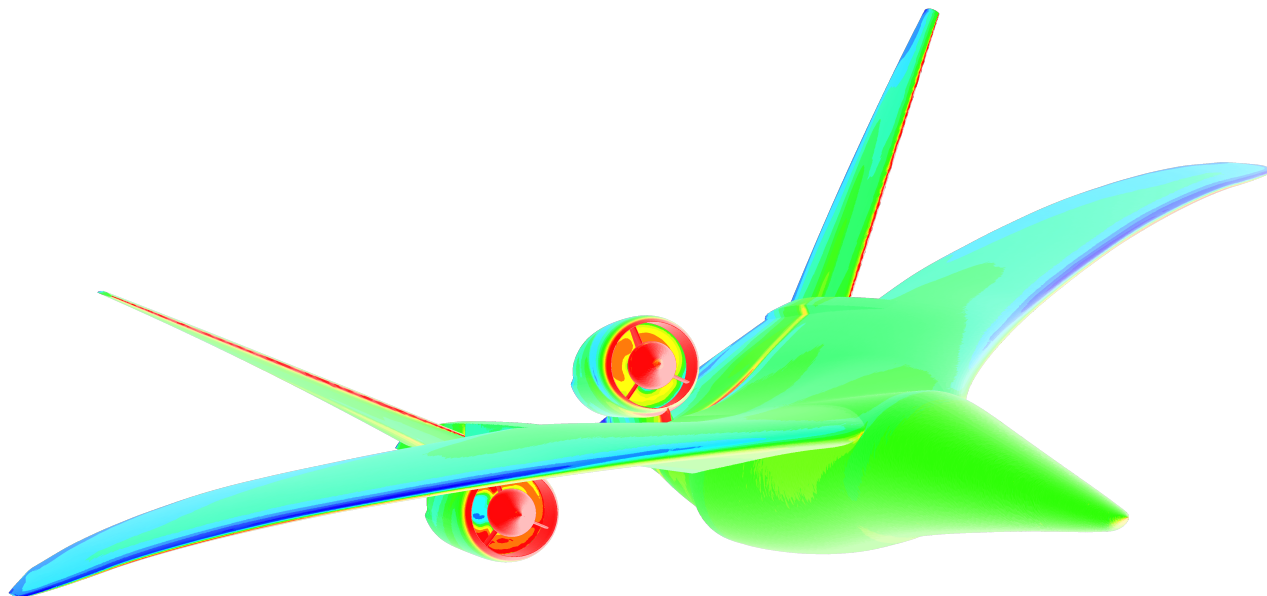


Figure 16. Fully integrated APSE model steady-state coefficient of pressure across vehicle and normalized total pressure at the engine face.

VII. Future Work

Currently, only steady-state results have been presented for the fully integrated propulsion system and N+2 vehicle, however dynamic models will be required for the APSE model. While there is no experimental data to verify the computational results of such a model, the simple quasi-1D model will be used to provide some comparative results. In addition, mesh refinement studies are required for greater confidence that the models are capturing the relevant physics. Once confidence is gained in the current rigid body model, the aero-elastic modes of the vehicle will need to be included to perform static aero-elastic studies of the full APSE model.

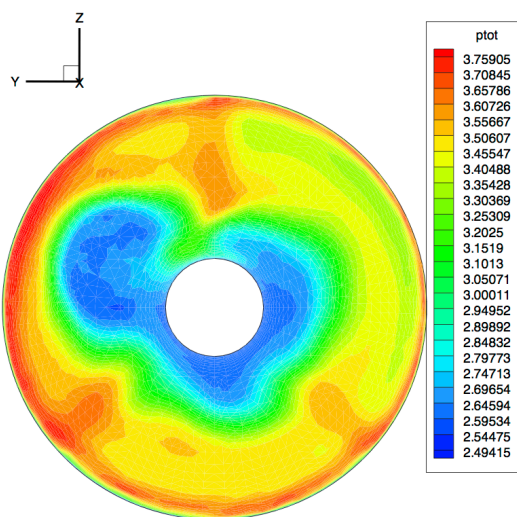


Figure 17. Fully integrated APSE model steady-state normalized total pressure profile at the engine face for the wing mounted propulsion system.

VIII. Conclusions

An integrated propulsion system component model has been developed, which is suitable for incorporation into an overall supersonic vehicle aero-propulso-servo-elastic (APSE) model where accurate thrust dynamics are of primary concern. The individual component modeling methodology was compared against steady and dynamic test data where available and compared against high fidelity models when no test data exists. Perturbations in the free stream flow field are applied that are in the frequency range of the expected atmospheric turbulence. The thrust oscillation obtained from the atmospheric disturbances was compared to the method previously done with only the engine component. The integrated propulsion system exhibits a more complex transient response indicating the need for the coupling of the full propulsion system to be studied. The atmospheric turbulence applied here was moderate, but the expectation of more severe turbulence will cause oscillations resulting in the aero-elastic modes of the vehicle to be impacted. The primary accomplishment of this study is the coupling between the simple propulsion system turbo-machinery model into a high fidelity computational fluid dynamics (CFD) model. The propulsion system model integrated into the higher fidelity CFD model was able to capture the main steady-state flow field about the propulsion system and enables future APSE studies.

Acknowledgments

The authors would like to thank David Friedlander for providing two dimensional model results for the nozzle and Mark Sanetrik for providing an unstructured grid of the N+2 concept vehicle.

References

- ¹AGARD, editor, *Advanced Aeroelasticity Testing and Data Analysis*, No. 566. NATO, 1995.
- ²Silva, W., Keller, D., Florance, J., and et. al., "Experimental Steady and Unsteady Aerodynamic and Flutter Results fo HSCT Semispan Models," *AIAA 41st Structures, Structural Dynamics, and Materials Conference*, No. AIAA 2000-1697, 2000.
- ³Biedron, R. T., Derlaga, J. M., Gnoffo, P. A., and et. al., "FUN3D Manual 12.4," Tech. Rep. TM-2014-218179, 2014.
- ⁴Silva, W., Sanetrik, M., Chwaloski, P., and Connolly, J., "Computational Aeroelastic Analysis of a Low-Boom Supersonic Configuration," *AIAA Aviation Forum*, 2015.
- ⁵Kopasakis, G., Connolly, J., and Seidel, J., "Propulsion System Dynamic Modeling of the NASA Supersonic Concept Vehicle for AeroPropulsoServoElasticity," *50th AIAA/ASME/SAE/ASEE Propulsion and Energy Forum*, No. AIAA 2014-3684, 2014.
- ⁶Garrard, D., Davis, M., Wehofer, S., and Cole, G., "A One Dimensional, Time Dependent Inlet/Engine Numerical Simulation for Aircraft Propulsion Systems," *ASME International Gas Turbine Institutes Turbo Expo*, No. 97-GT-333, 1997.
- ⁷Garrard, D., "ATEC: The Aerodynamic Turbine Engine Code for the Analysis of Transient and Dynamic Gas Turbine Engine System Operations Part 1: Model Development," *ASME International Gas Turbine Institutes Turbo Expo*, No. 96-GT-193, 1996.
- ⁸Garrard, D., "ATEC: The Aerodynamic Turbine Engine Code for the Analysis of Transient and Dynamic Gas Turbine Engine System Operations Part 2: Numerical Simulations," *ASME International Gas Turbine Institutes Turbo Expo*, No. 96-GT-194, 1996.
- ⁹Gamble, E., Haid, D., D'Alessandro, S., and DeFrancesco, R., "Dual-Mode Scramjet Performance Model for TBCC Simulation," *45th AIAA/ASME/SAE/ASEE Joint Propulsion Conference and Exhibit*, No. AIAA 2009-5298, 2009.
- ¹⁰Numbers, K. and Hamed, A., "Development of a Coupled Inlet-Engine Dynamic Analysis Method," *33rd AIAA/ASME/SAE/ASEE Joint Propulsion Conference and Exhibit*, No. AIAA-1997-2880, 1997.
- ¹¹Giannola, P., Haas, M., Cole, G., and Melcher, K., "Modeling the Dynamics of Superonic Inlet/Gas Turbine Engine Systems for Large - Amplitude High Frequency Disturbances," *36th AIAA/ASME/SAE/ASEE Joint Propulsion Conference and Exhibit*, No. A00-36772, 2000.
- ¹²Clark, A., Wu, C., Mirmirani, M., and Choi, S., "Development of an Airframe-Propulsion Integrated Generic Hypersonic Vehicle Model," *46th AIAA Aerospace Sciences Meeting and Exhibit*, No. AIAA 2006-218, Reno, Nevada, 9-12 January 2006.
- ¹³Rudd, L. and Pines, D., "Integrated Propulsion Effects on Dynamic Stability and Control of Hypersonic Waveriders," No. AIAA 2000-3826, July 2000.
- ¹⁴Raney, D. L., McMinn, J. D., Potozky, A., and Wooley, C. L., "Impact of Aeroelasticity on Propulsion and Longitudinal Flight Dynamics of an Air-Breathing Hypersonic Vehicle," No. AIAA 1993-1367, 1993.
- ¹⁵Connolly, J., Kopasakis, G., Paxson, D., Stueber, E., and Woolwine, K., "Nonlinear Dynamic Modeling and Controls Development for Supersonic Propulsion System Research," *47th AIAA/ASME/SAE/ASEE Joint Propulsion Conference and Exhibit*, No. AIAA-2011-5653, 2011.
- ¹⁶Kopasakis, G., Connolly, J., and Kratz, J., "Quasi One-Dimensional Unsteady Modeling of External Compression Supersonic Inlets," *48th AIAA/ASME/SAE/ASEE Joint Propulsion conference*, No. AIAA 2012-4147, 2012.
- ¹⁷Anderson, J., "Computational Fluid Dynamics: The Basics with Applications," McGraw Hill, New York, NY, 1995.
- ¹⁸Giles, M., "Nonreflecting Boundary Conditions for Euler Equations Calculations," *AIAA Journal*, Vol. 28, No. 12, 1989.

- ¹⁹Chima, R., Conners, T., and Wayman, T., "Coupled Analysis of an Inlet and Fan for a Quiet Supersonic Jet," *48th AIAA Aerospace Sciences Meeting*, No. AIAA 2010-479, 2010.
- ²⁰Kopasakis, G., "Feedback Control Systems Loop Shaping Design with Practical Considerations," Tech. rep., NASA TM 2007-215007, September 2007.
- ²¹Kopasakis, G., Connolly, J., Paxson, D., and Ma, P., "Volume Dynamics Propulsion System Modeling for Supersonics Vehicle Research," *Journal of Turbomachinery*, Vol. 132, No. 4, October 2010, pp. 25–33.
- ²²Seldner, K., Mihalow, J., and Blaha, R., "Generalized Simulation Technique for Turbojet Engine System Analysis," Tech. rep., NASA TN-D-6610, 1972.
- ²³Lytle, J. K., "The Numerical Propulsion System Simulation: A Multidisciplinary Design System for Aerospace Vehicles," Tech. rep., NASA TM 1999-209194, 1999.
- ²⁴Horowitz, I., "Quantitative Feedback Theory," *IEEE Proceedings*, Vol. 129, No. 6, Nov. 1982, pp. 215–226.
- ²⁵Connolly, J. and Kopasakis, G., "Loop Shaping Control Design for a Supersonic Propulsion System Model Using QFT Specifications and Bounds," *46th AIAA/ASME/SAE/ASEE Joint Propulsion Conference and Exhibit*, No. AIAA-2010-7086, 2010.
- ²⁶Kopasakis, G., "Atmospheric Turbulence Modeling for Aero Vehicles: Fractional Order Fits," Tech. rep., NASA TM 2010-216961, Jan. 2010.
- ²⁷Kopasakis, G., "Modeling of Atmospheric Turbulence as Disturbances for Control Design and Evaluation of High Speed Propulsion Systems," *Journal of Dynamic Systems, Measurement, and Control*, Vol. 134, No. 021009, 2011, pp. 74–86.
- ²⁸Connolly, J., Friedlander, D., and Kopasakis, G., "Computational Fluid Dynamics Modeling of a Supersonic Nozzle and Integration into a Variable Cycle Engine Model," *50th AIAA/ASME/SAE/ASEE Joint Propulsion conference*, No. AIAA 2014-3687, 2014.
- ²⁹Friedlander, D. and Wang, X.-Y., "Steady and Unsteady Nozzle Simulations Using the Conservation Element and Solution Element Method," *50th AIAA/ASME/SAE/ASEE Joint Propulsion conference*, No. AIAA-2014-4014, 2014.
- ³⁰Carlson, J.-R., "Inflow/Outflow Boundary Conditions with Application to FUN3D," Tech. rep., NASA TM 2011-217181, 2011.
- ³¹Whiting, C. H. and Jansen, K. E., "A Stabilized Finite Element Method for the Incompressible Navier-Stokes Equations Using a Hierarchical Basis," *International Journal for Numerical Methods in Engineering*, Vol. 35, 2001, pp. 93–116.
- ³²Chang, S.-C., "The Method of Space-Time Conservation Element and Solution Element - A New Approach for Solving the Navier-Stokes and Euler Equations," Tech. rep., NASA TM-111237, 1995.